

Original Article

The residue I257 at S4–S5 linker in KCNQ1 determines KCNQ1/KCNE1 channel sensitivity to 1-alkanols

Chang XIE^{1, #}, Hao-wen LIU^{2, #}, Na PAN², Jiu-ping DING², Jing YAO^{1, *}¹College of Life Sciences, Wuhan University, Wuhan 430072, China; ²Key Laboratory of Molecular Biophysics of the Ministry of Education, College of Life Science and Technology, Huazhong University of Science and Technology, Wuhan 430074, China

Aim: KCNQ1 and KCNE1 form a complex in human ventricular cardiomyocytes, which are important in maintaining a normal heart rhythm. In the present study we investigated the effects of a homologous series of 1-alkanols on KCNQ1/KCNE1 channels expressed in *Xenopus* oocytes.

Methods: ECG recording was made in rats injected with ethanol-containing solution (0.3 mL, ip). Human KCNQ1 channel and its auxiliary subunit KCNE1 were heterologously coexpressed in *Xenopus* oocytes, which were superfused with ND96 solution; 1-alkanols (ethanol, 1-butanol and 1-hexanol) were delivered through a gravity-driven perfusion device. The slow-delayed rectifier potassium currents I_{Ks} (KCNQ1/KCNE1 currents) were recorded using a two-electrode voltage clamp method. Site-directed mutations (I257A) were made in KCNQ1.

Results: In ECG recordings, a low concentration of ethanol (3%, v/v) slightly increased the heart rate of rats, whereas the higher concentrations of ethanol (10%, 50%, v/v) markedly reduced it. In oocytes coexpressing KCNQ1/KCNE1 channels, ethanol, 1-butanol and 1-hexanol dose-dependently inhibited I_{Ks} currents with IC_{50} values of 80, 11 and 2.7 mmol/L, respectively. Furthermore, the 1-alkanols blocked the KCNQ1 channel in both open and closed states, and a four-state model could adequately explain the effects of 1-alkanols on the closed-state channel block. Moreover, the mutation of I257A at the intracellular loop between S4 and S5 in KCNQ1 greatly decreased the sensitivity to 1-alkanols; and the IC_{50} values of ethanol, 1-butanol and 1-hexanol were increased to 634, 414 and 7.4 mmol/L, respectively. The mutation also caused the ablation of closed-state channel block.

Conclusion: These findings provide new insight into the intricate mechanisms of the blocking effects of ethanol on the KCNQ1 channel.

Keywords: KCNQ1; KCNE1; I_{Ks} current; ethanol; 1-butanol; 1-hexanol; closed-state channel block; open channel block

Acta Pharmacologica Sinica (2016) 37: 124–133; doi: 10.1038/aps.2015.133

Introduction

Ethanol has a wide range of pharmacological effects on the human body, and the enormous socioeconomic burden of its abuse has led to long and intense efforts to define the mechanism of its action. Ion channels and receptors in the nervous systems are associated with the acute physiological effect of ethanol. Ligand-gated ion channels activated by neurotransmitters, including GABA, glycine, glutamate, acetylcholine, serotonin, and purines, are all affected by ethanol. For example, intoxicating concentrations (5–50 mmol/L) of ethanol can

facilitate GABA_A receptor activity but inhibit NMDA receptor function, thus affecting the activity of neurons. Ethanol and many other anesthetics may directly or indirectly target one or more membrane proteins^[1–3]; however, the underlying mechanisms that mediate its actions are still poorly understood^[4–6].

To date, many studies have documented that the functions of a variety of ion channels, receptors and transporters are altered by ethanol^[6]. The effects of ethanol on ion channels are diverse. For instance, Covarrubias *et al* previously reported that moderate concentrations of ethanol (17–170 mmol/L) selectively inhibited a non-inactivating cloned potassium channel encoded by *Drosophila* Shaw^[7, 8]. Cavaliere *et al* demonstrated that the *Drosophila* KCNQ channel is more sensitive to ethanol than the mammalian KCNQ2/3 channel^[9]. Clinically relevant concentrations of ethanol (10–100

[#] These authors contributed equally to this work.

^{*} To whom correspondence should be addressed.

E-mail jyao@whu.edu.cn

Received 2015-09-14 Accepted 2015-11-10

mmol/L) rapidly and reversibly potentiated the activity of BK channels in excised patches of the neurohypophysial terminal membrane and in oocytes expressing cloned BK channels, and several dominant binding sites have been identified^[1, 6, 10-15]. Human Kv1.5 channel currents were also inhibited by ethanol in HEK293 cells^[16]. In addition, several laboratories have found that ethanol targets G-protein-gated inwardly rectifying potassium (GIRK) channels in the brain^[17-21]. Interestingly, the transient receptor potential vanilloid 1 (TRPV1) can be directly activated by ethanol, and its responses to different stimuli also can be potentiated by ethanol^[22]. Recently, Vigna *et al* reported that ethanol contributes neurogenic pancreatitis by activating the TRPV1 channel^[23]. Biochemical and electrophysiological approaches have demonstrated the presence of ethanol-binding sites in various ion channel proteins, but there remains a considerable debate regarding the putative binding sites due to a lack of 3D structural data^[7, 8, 24].

Ethanol has been reported to affect the human heart rate^[25, 26]. KCNQ1 and KCNE1 form a complex in human ventricular cardiomyocytes and are involved in recharging the cardiac muscle after each heartbeat to maintain a regular rhythm. Loss-of-function mutations in the KCNQ1 gene cause hereditary long QT syndrome due to the reduction of the repolarizing potassium cardiac current. Given the importance of the KCNQ1 channel in the formation and propagation of cardiac action potential^[27-30], we sought to investigate whether ethanol has an effect on the KCNQ1 channel. In the present study, we report that a homologous series of 1-alkanols (ethanol, 1-butanol and 1-hexanol) could inhibit I_{Ks} (KCNQ1/KCNE1) currents in *Xenopus* oocytes in a concentration-dependent manner. Considering the importance of hydrophobic interaction during the binding of 1-alkanols to channel polypeptides, our results revealed that the inhibition potency was enhanced with increasing alkyl chain length from C2 to C6. Our results suggest that 1-alkanols could interact with the KCNQ1 channel in both the open and closed states. In addition, we demonstrated that a four-state model was able to globally fit the responses under all circumstances. Furthermore, we identified a critical residue, I257, within the intracellular loop between transmembrane segments 4 and 5 of the KCNQ1 channel that played a key role in the inhibition of KCNQ1/KCNE1 channels in the active pre-open state.

Materials and methods

Mutagenesis and expression

Full-length cDNA for human KCNQ1 was subcloned into PCI-CMCiso. All of the mutations were generated using the TransformerTM Site-directed Mutagenesis Kit, as described by the manufacture (Clontech, Mountain View, CA, USA). The resulting mutations were verified by restriction enzyme digestion and DNA sequencing. After the cDNA was linearized, SP6 RNA polymerase (Roche Applied Science, Indianapolis, IN, USA) was used to synthesize capped cRNA for microinjection. The final cRNA was resuspended in RNase-free water and stored at -80 °C.

Xenopus laevis oocytes were defolliculated by treat-

ment with 2 mg/mL collagenase I (Sigma-Aldrich, St Louis, MO, USA) in Ca²⁺-free ND96 solution as previously described^[31]. With a Drummond Nanoject II injector (Drummond Scientific Co, Broomall, PA, USA), 5–10 ng of cRNA was injected into stage V–VI *Xenopus* oocytes. In order to maintain KCNE1 subunits at a saturating concentration, we co-injected KCNQ1 and KCNE1 mRNAs into oocytes at a ratio of at least 1:2 by molecular weight. After injection, oocytes were then incubated in ND96 solution supplemented with 2.5 mmol/L sodium pyruvate, 100 U/mL penicillin and 100 µg/mL streptomycin at 18 °C for 2–7 days. The ND96 solution for oocytes consisted of (in mmol/L) the following: 96 NaCl, 2 KCl, 1.8 CaCl₂, 1 MgCl₂ and 10 H⁺-HEPES, pH 7.4 (adjusted with NaOH).

Electrophysiology

Currents were recorded at room temperature (22–25 °C) 2–3 days after cRNA injection. Two-electrode voltage-clamp measurements with the commercially available amplifier TURBO TEC-03X (NPI electronic GmbH, Hauptstrasse 96, D-71732 Tamm, Germany) and pClamp9 software (Molecular Devices, Sunnyvale, CA, USA) were obtained at steady state, typically 2–3 min after drug application. Patch pipettes that were pulled from borosilicate glass capillaries had resistances of 0.5–1.0 MΩ when filled with 3 mol/L KCl solution. Currents were recorded in ND96 solution, and the holding potential was -30 mV. Unless stated otherwise, following the voltage protocol for current recordings from a holding potential of -30 mV, the cells were pulsed to voltages between -60 mV and +60 mV in steps of 10 mV for 3 s, followed by a 1-s test pulse to -120 mV. During recording, the oocytes were regularly perfused with standard recording solution, after which 1-alkanols (C2, C4, and C6), such as ethanol, 1-butanol and 1-hexanol (diluted in the appropriate external solutions to the desired final concentrations immediately before use), were applied through a gravity-driven perfusion device at 4 mL/min or greater. Then, the solution equilibration currents were typically digitized and filtered at 2 and 1 kHz, respectively.

ECG recording

Male Wistar rats weighing 200–250 g were obtained from an animal house in the Hubei Provincial Center for Disease Control and Prevention (Wuhan, China) and housed under controlled environmental conditions of 20–25 °C, 50%–55% relative humidity, and 12-h light/dark cycle with free access to stock laboratory diet and water. After the induction of anesthesia, a set of different concentrations of ethanol (diluted in normal saline solution) or normal saline (as control) was then injected into the abdomen of rats, and approximately 40 min later, the HR (heart rate) data were obtained and analyzed by the Medlab system, which was connected to the rat's external tail, where the pulse was detected following the manufacturer's instructions. Once the experiments were completed, the animals were allowed to wake gently and then individually housed in a standard rat cage until their health condition was assured.

Data analysis

Data were analyzed with SigmaPlot software (SPSS Inc, USA) and Clampfit 9.0 software (Axon Instruments Inc, USA). Unless otherwise stated, all of the data are presented as the mean±SEM. n is the number of individual oocytes that were tested for each experiment. Statistical analyses were performed with Student's t -test using SigmaPlot. $P < 0.05$ was considered statistically significant. Conductance-voltage (G - V) curves for activation were derived from peak currents at test potentials ranging from -60 to $+60$ mV for 3 s. The obtained data were fit with a Boltzmann function:

$$G/G_{\max} = a / \{ [1 + \exp(V - V_{50})/k] \times [1 - \exp(V - V_{50})/k] \} \quad (1)$$

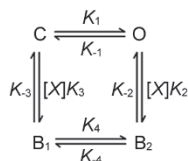
where V_{50} is the voltage of the half-maximal activation of conductance, and k is the slope factor. Dose-response curves for activation were derived from peak currents at test potentials ranging from -60 mV to $+60$ mV for 3 s. The obtained data were fit with the Hill equation:

$$I/I_{\max} = 1 / (1 + (IC_{50}/[\text{drug}])^n) \quad (2)$$

where IC_{50} represents the concentration of the half-maximal blocking of the drug, and n is the Hill coefficient.

Block of both open and closed states

Model I (CB-OB model) was used to evaluate whether a blocker may act by binding to the same site in both open and closed states^[32, 33].



Model I

For Model I, the predictions of P_o as a function of voltage and blocker concentration $[X]$ are:

$$P_o = 1 / (1 + K_{-1}/K_1 + K_{-1}/K_1 \times K_3/K_3 \times [X] + K_2/K_2 \times [X]) \quad (3)$$

where K_{-3}/K_3 denotes the $K_{BC} \times \exp(-z_b \cdot FV)/RT$, and Equation 3 yields the following well-known expression for the dependence of conductance on voltage and blocker:

$$G(V, [X]) = G_{\max} / (1 + \exp(-qF(V - V_{50}))/RT + (\exp(-qF(V - V_{50}))/RT) \times [X] / (K_{BC} \times \exp(-z_b \cdot FV)/RT) + [X] / (K_{BO} \times \exp(-z_b \cdot FV)/RT))$$

where q is the valence that is associated with the activation equilibrium; V_{50} is the voltage of half-activation; K_{BO} and K_{BC} are the 0-voltage dissociation constants of blocker X for the open or closed state, respectively, with z_b reflecting the intrinsic voltage dependence of the binding equilibrium; and R , T , and F are standard constants.

Open-channel block

Model II defines the basic open-channel blocking mechanism (OB model) with predictions for steady-state P_o defined in Equation 4.



$$P_o = 1 / (1 + K_{-1}/K_1 + K_2/K_2 \times [X]) \quad (4)$$

where K_{-1}/K_1 denotes the $\exp(-qF(V - V_{50}))/RT$, and K_2/K_2 is $K_{BO} \times \exp(-z_b \cdot FV)/RT$. Then, Equation 4 yields the following well-known expression for the dependence of conductance on voltage and blocker:

$$G(V, [X]) = G_{\max} / (1 + \exp(-qF(V - V_{50}))/RT + [X] / (K_{BO} \times \exp(-z_b \cdot FV)/RT))$$

where all of the variables have the same definition as described in Model I.

Results

Ethanol leads to the sinus bradycardia of rats

We first performed electrocardiogram (ECG) recordings to evaluate the effects of ethanol on the cardiovascular system in adult male Wistar rats. The different concentrations of ethanol

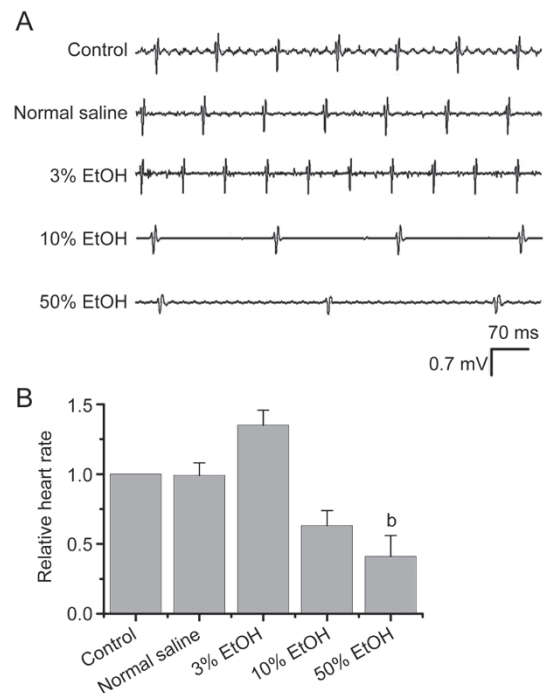


Figure 1. Electrocardiogram (ECG) changes in rats with acute ethanol treatments. (A) ECG recordings in adult male Wistar rats. Representative tracings of ECG recorded from individual rat before and after injection with 0.3 mL of normal saline or a solution containing 3%, 10% or 50% ethanol (v/v). Each solution was injected into the abdomen of a different rat fixed by two cortical electrodes. The proper position of ECG leads was monitored by the telemetry signal quality using the recording software, and all of the ECG traces were recorded until the quality of the ECG signal was considered acceptable, usually approximately 40 min after each treatment for an individual rat. The ~1-s ECG recordings were mainly used for average heart rate measurements, albeit the voltage amplitude values being remarkably reduced, especially in the rats that were injected with high concentrations of ethanol (eg, 50%). (B) Comparison of heart rate responses to different treatments ($n=3-6$). Mean±SEM. ^b $P < 0.05$ vs control. EtOH, ethanol.

were injected into the abdomen of rats fixed using two cortical electrodes. Figure 1A illustrates the ECG recordings from different rats, showing that the heart rate was slightly faster when injected with the lower concentration of ethanol (3%, v/v) but was significantly reduced with an increasing concentration of ethanol compared to the control group or to that injected with normal saline. Although the voltage amplitude values were remarkably reduced, especially in the rats that were injected with higher concentrations of ethanol (eg, 50%), the ECG recordings in this study were mainly used for average heart rate measurements due to the broad effects of ethanol on ion channels. For example, it has been suggested that ethanol has an acute inhibitory effect on the gating of sodium channels in the heart^[34]. Figure 1B summarizes the different effects of ethanol at various concentrations on the heart rate. The changes in ECG indicate that ethanol may enhance the hyperpolarization-activated cation (I_h) currents in sinus pacemaker cells to speed up the heartbeat at lower concentrations (3% ethanol) through a signal transduction pathway, eg, ethanol increases the larger-conductance Ca^{2+} -activated K^+ (I_{BK}) currents to release more norepinephrine (NE) in chromaffin cells to stimulate the β -adrenergic receptors to increase I_h currents in pacemaker cells to speed up the heart beat^[35,36]. In contrast, a relatively high concentration of ethanol (eg, 10% or 50%) might inhibit the I_{Ks} (KCNQ1/KCNE1) currents to prolong the duration of action potentials to slow down the heartbeat, which will be further illustrated by the following experiments.

Alkyl chain length determines the blocking efficiency of 1-alkanols on the KCNQ1/KCNE1 channel

To discern whether ethanol affects the I_{Ks} (KCNQ1/KCNE1) currents, we used two-electrode voltage-clamp technology to identify the pharmacological sensitivity of the channel to various members of the homologous series of 1-alkanols (C2, C4, and C6), such as ethanol, 1-butanol and 1-hexanol. The different concentrations of 1-alkanols were prepared and applied externally as described in the Materials and Methods section. The bath solution was continuously exchanged at 3–4 mL/min or greater to ensure the attainment of equilibrium. Figure 2A shows representative current traces resulting from a family of voltage steps either under control conditions or in the presence of ethanol (200 mmol/L), 1-butanol (50 mmol/L) or 1-hexanol (5 mmol/L). With voltage steps from -60 to $+60$ mV in 10-mV increments for 3 s, during which the current was stable, the I_{Ks} (KCNQ1/KCNE1) currents were remarkably suppressed with extracellular applications of ethanol, 1-butanol or 1-hexanol. Note that the I_{Ks} currents could be fully recovered after washing away the 1-alkanols. Figure 2B shows plots of relative currents vs voltage, demonstrating that ethanol, 1-butanol and 1-hexanol are inhibitors of KCNQ1/KCNE1 channels. The inhibition effects of all three 1-alkanols on I_{Ks} currents were increased in a concentration-dependent manner. Furthermore, we found that the inhibition potency was enhanced along with extending alkyl chain length from C2 to C6. For example, the application of 10 mmol/L 1-hexanol caused a $53\% \pm 2\%$ reduc-

tion of I_{Ks} currents at $+40$ mV ($n=6$), but only $32\% \pm 3\%$ and $28\% \pm 5\%$ reductions for 10 mmol/L 1-butanol ($n=7$) and 10 mmol/L ethanol ($n=5$), respectively.

1-Alkanols inhibit I_{Ks} currents of KCNQ1 channels in both open- and closed-state

Because each blocking effect of ethanol, 1-butanol or 1-hexanol on I_{Ks} currents was reversible, we examined them in more mechanistic detail. Figure 3A shows the concentration-response curves of the inhibitory effects of ethanol (Figure 3A1), 1-butanol (Figure 3A2) and 1-hexanol (Figure 3A3) on I_{Ks} currents activated at a testing voltage of $+60$ mV. The respective IC_{50} values were estimated as 80 ± 2 mmol/L for ethanol ($n=4$), 11 ± 2 mmol/L for 1-butanol ($n=5$) and 2.7 ± 1.7 mmol/L for 1-hexanol ($n=5$), showing that the IC_{50} values decreased by approximately 5-fold or 20-fold as the alkyl chain length increased from C2 to C4 or C6. These results further demonstrate that extending the alkyl chain length would accordingly increase the inhibition efficiency of 1-alkanols on I_{Ks} currents, which is also consistent with the previous report by Covarrubias^[8]. As illustrated in Figure 3B, all three 1-alkanols exhibited a slightly stronger inhibition of I_{Ks} currents evoked at lower voltages. The hydrophobicity of the alkanol will be consequently increased upon increasing the alkyl side chain length. These results suggest that both the hydrophobic chains and voltage are important for responses of the KCNQ1/KCNE1 channels to 1-alkanols, to both of which hydrophobic interactions are major contributing factors.

To assess whether the blocking of each alkanol is time dependent, Figure 3C compared the fractional inhibition curves along with elapsed time at a testing potential of $+60$ mV. The inhibition varied during the channel opening duration (from the transient beginning to the steady state); thus, in the beginning, I_{Ks} currents elicited at $+60$ mV were blocked by more than 60% with the application of 200 mmol/L ethanol. However, the blocking ratio decreased to a stable value of approximately 40% as more channels opened. The results shown in Figure 3C indicate a closed-state block for ethanol, 1-butanol or 1-hexanol in addition to the open-channel block. To obtain a complete description of the closed-state block, I_{Ks} currents evoked at $+60$ mV were measured at the active pre-open state (at the time point of 100 ms during opening) before and after treatment with 1-alkanols. This measurement yielded a sigmoidal concentration-response curve for the closed-state block (Figure 3D). Fitting the data points with the Hill equation resulted in $IC_{50} = 58 \pm 0.8$ mmol/L for ethanol ($n=4$), 23 ± 2 mmol/L for 1-butanol ($n=5$) and 5 ± 0.8 mmol/L for 1-hexanol ($n=5$). The steepness of the curves remained largely unchanged (ethanol: n_H of ~ 0.5 ; 1-butanol: n_H of ~ 0.5 ; and 1-hexanol: n_H of ~ 0.5). Figure 3E summarizes plots of peak conductance vs voltage. Next, to obtain insight into the closed-state channel blocking, we found that a four-state block model (Model I), as described in the Materials and methods section, was able to adequately fit the responses globally under all circumstances, and the solid lines represent the best fits. The model-based fittings of the closed-state channel block yielded

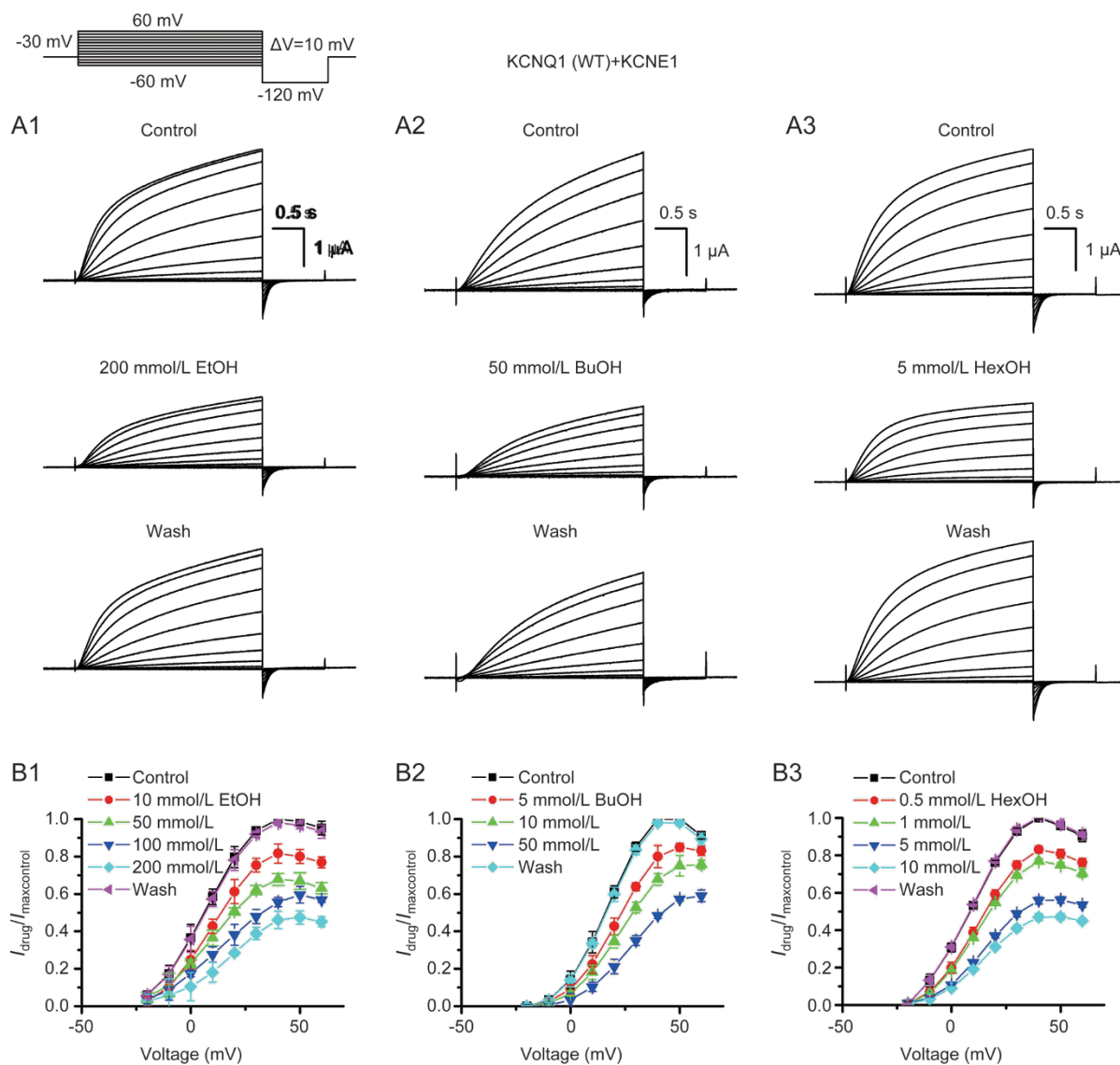


Figure 2. Extending the alkyl chain length augments the inhibition efficiency of 1-alkanols on I_{Ks} currents as recorded in oocytes. (A) Representative currents were recorded from oocytes expressing wild-type KCNQ1/KCNE1 under two-electrode voltage-clamp by voltage steps from -60 to $+60$ mV in 10 -mV increments lasting for 3 s in the presence and absence of 200 mmol/L ethanol (termed as EtOH; A1), 50 mmol/L 1-butanol (BuOH; A2) and 5 mmol/L 1-hexanol (HexOH; A3) as indicated. Voltage protocols included above current traces. (B) Summary plots of I - V curves before and after exposure to different concentrations of EtOH (B1; $n=4$), BuOH (B2; $n=5$) and HexOH (B3; $n=5$) as indicated. All of the currents at each concentration were normalized to their respective control values.

$IC_{50} = 60.8 \pm 0.8$ mmol/L for ethanol, 17.6 ± 2 mmol/L for 1-butanol and 1.6 ± 0.8 mmol/L for 1-hexanol, and these values were similar to those previously derived from the sigmoidal curve fits. Evidence from the adequate model fitting thus confirms that 1-alkanols could block the KCNQ1/KCNE1 channel in both open and closed states.

I257 is a critical residue for 1-alkanols binding to the KCNQ1 channel

Interestingly, the *C. elegans* kqt-3/KCNE1 channel was less sensitive to ethanol compared to the KCNQ1 channel (Figure 4A and B), which might be due to some different key amino acids between kqt-3 and KCNQ1. In addition, the S4-S5 linker

confers the modulation of the Shaw2 K^+ channel by 1-alkanols, indicating that this conserved region of the K^+ channel might play an essential role in interacting with 1-alkanols^[8]. We thus performed a sequence alignment of the S4-S5 region where the ethanol binding pocket might be located between *C. elegans* kqt-3 and human KCNQ1. Based on the sequence alignment, we found four different amino acids (Figure 4C). We previously reported that hydrophobicity has a remarkable effect on the affinity of 1-alkanol to the KCNQ1 channel (Figure 2), providing clear evidence that hydrophobic interactions might contribute greatly to the binding of 1-alkanols. As inferred from the hydrophobicity analysis of amino acids, we found that the most notable residue in the linker of S4-S5 was I257 in

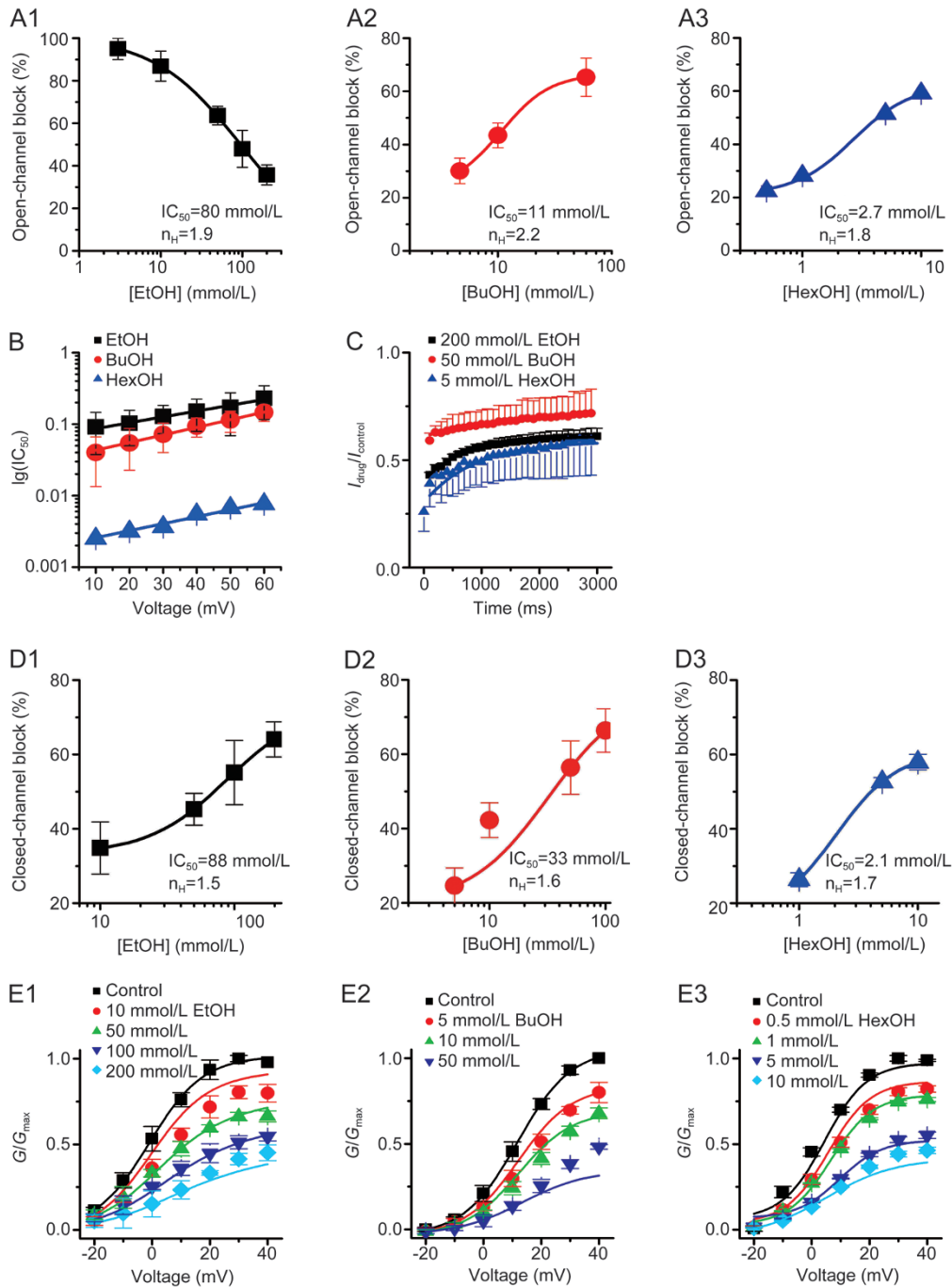


Figure 3. 1-Alkanols inhibit I_{Ks} currents in both the open and closed state of wild-type KCNQ1/KCNE1 channels. (A) Dose-response curves for the open-channel block were plotted for EtOH (A1; $n=4$), BuOH (A2; $n=5$) and HexOH (A3; $n=5$) at +20 mV and were fitted to the Hill equation. Both the IC_{50} values and the corresponding Hill coefficient n_H are indicated on each panel. (B) Voltage-dependence of IC_{50} values for EtOH ($n=4$), BuOH ($n=4$) and HexOH ($n=3$). The solid lines are the lines of best fit of the function $k(V)=k(0)\times\exp(-zFV/RT)$, where $k(0)$ represents the IC_{50} for 1-alkanols at 0 mV, and z is the fitted value for fractional charges moved during block reaction. The variables of F , R and T have their standard definitions. For EtOH, $k(0)=0.0718$ with $z=-0.4749$; $k(0)=0.0338$ with $z=-0.6200$ for BuOH; and $k(0)=0.0021$ with $z=-0.5688$ for HexOH. (C) Time courses and fractional inhibitions of KCNQ1/KCNE1 currents evoked at +60 mV in the presence of 200 mmol/L EtOH ($n=4$), 50 mmol/L BuOH ($n=4$) and 5 mmol/L HexOH ($n=5$). (D) Dose-dependence of three 1-alkanols effects on the closed state KCNQ1 channels. The inhibition values or ratios by 1-alkanols at the closed state were derived from the values at the intersection of the prolonged line of $I_{drug}/I_{control}$ and the zero time axis ($t=0$ s), as shown in Figure 3C. The solid line represents a Hill equation fit. (E) Normalized conductance-voltage relationship. The conductances that were obtained from steady state currents at the end of the pulse in the presence of various concentrations of EtOH (E1), BuOH (E2) and HexOH (E3) were simultaneously fit to a four-state block model (Model I) as described in the main text (solid lines). The optimal fit for the open and closed-channel block (OB-CB) yielded $K_{OB}=90\pm 8.2$ mmol/L, $K_{CB}=60.8\pm 7.0$ mmol/L for EtOH (E1), $K_{OB}=20\pm 5.2$ mmol/L, $K_{CB}=17.6\pm 6.1$ mmol/L for BuOH (E2) and $K_{OB}=5.0\pm 2.1$ mmol/L, $K_{CB}=1.6\pm 1.5$ mmol/L for HexOH (E3). The error bars represent the SEM. EtOH, ethanol; BuOH, 1-butanol; HexOH, 1-hexanol.

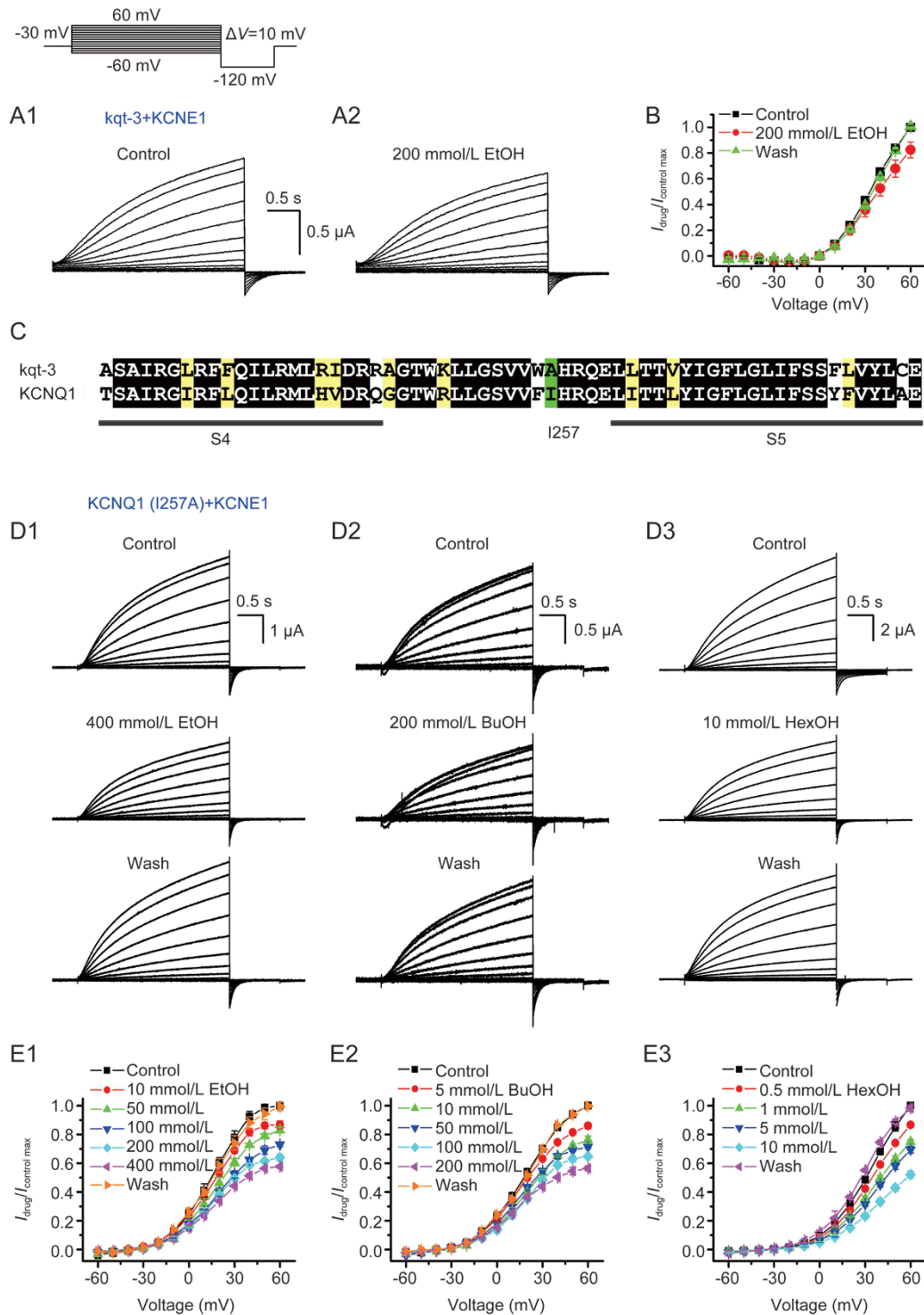


Figure 4. I257, the residue in the intracellular linker of transmembranes S4 and S5, is critical for the 1-alkanol inhibition of KCNQ1 channels. (A) Effects of ethanol on *kqt-3* currents. Representative outward current in oocytes expressed with *kqt-3* and KCNE1 were evoked by step depolarizations from -90 mV to $+60$ mV in 10 -mV increments in the presence and absence of 200 mmol/L EtOH. The interpulse interval was 3 s. Voltage protocols are presented above current traces. (B) Summary plots of relative currents over voltage before and after exposure to different concentrations of EtOH ($n=4$), showing that ethanol (200 mmol/L) has a slight effect on *kqt-3* currents. (C) An amino acid alignment of the linker of S4 and S5 between *C. elegans* *kqt-3* and human KCNQ1. (D) Representative current traces from oocytes that were injected with KCNQ1 (I257A) and KCNE1 in response to voltage steps from -60 to $+60$ mV in 10 -mV increments for 3 s in the presence and absence of 400 mmol/L EtOH (D1), 200 mmol/L BuOH (D2) and 10 mmol/L HexOH (D3) as indicated. (E) Summary plots of relative current over voltage before and after exposure to different concentrations of EtOH (E1; $n=4$), BuOH (E2; $n=5$) and HexOH (E3; $n=5$) as indicated. All of the currents at each concentration were normalized to their respective control values. The error bars indicate the SEM. EtOH, ethanol; BuOH, 1-butanol; HexOH, 1-hexanol.

KCNQ1, whereas the corresponding residue was Ala in *kqt-3*. We thus focused on residue I257 in the linker of KCNQ1 and mutated it to the counter residue of *kqt-3*. The resultant mutation was designated as KCNQ1(I257A). Upon the expression of KCNQ1(I257A) with KCNE1 in oocytes, the mutant channel also exhibited an activation profile similar to that of the wild-type channel, as evoked by the same voltage protocol (Figure 4D). As expected, the mutation of I257A reduced the KCNQ1 channel sensitivity to ethanol (400 mmol/L; Figure 4D1 mid-

dle), 1-butanol (200 mmol/L; Figure 4D2 middle) and 1-hexanol (10 mmol/L; Figure 4D3 middle). Figure 4E shows plots of relative currents *vs* test potential (*I-V* curves) under different treatments. A statistical analysis revealed that the percentage of blockage for I257A decreased to $36\% \pm 2\%$, $28\% \pm 1\%$, and $30\% \pm 2\%$ by the application of 200 mmol/L ethanol, 50 mmol/L 1-butanol, and 5 mmol/L 1-hexanol, respectively. In contrast, wild-type I_{Ks} currents decreased to $55\% \pm 2\%$, $41\% \pm 3\%$, and $47\% \pm 1\%$ with the application of 200 mmol/L ethanol, 50

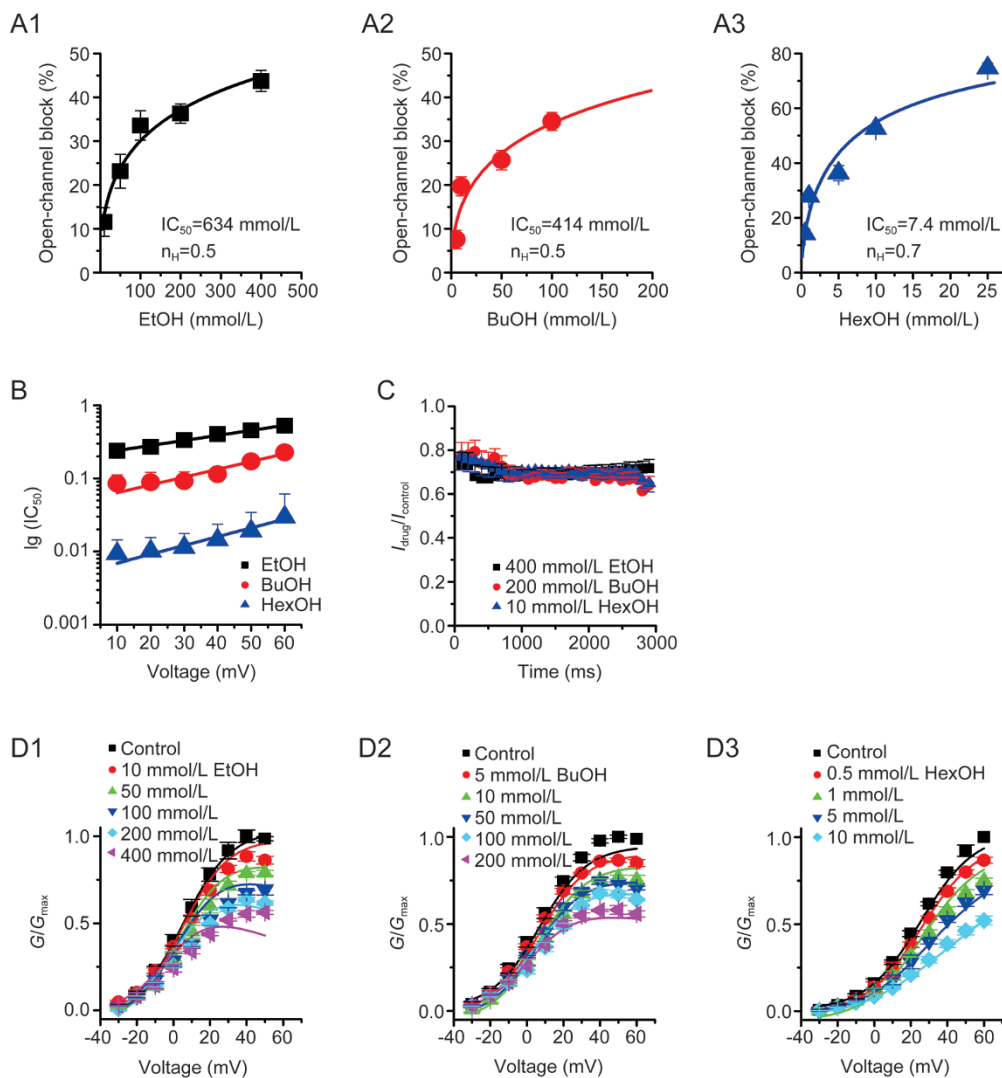


Figure 5. Substitution of I257 by alanine abrogates the closed-state block of the KCNQ1 channel by 1-alkanols. (A) Dose-response curves for the open-channel block by 1-alkanols; best fitting by Hill's equation resulted in the following: $IC_{50}=634 \pm 0.8$ mmol/L, $n_H=0.5$ for EtOH (A1, $n=5$); $IC_{50}=414 \pm 7.0$ mmol/L, $n_H=0.5$ for BuOH (A2, $n=5$); and $IC_{50}=7.4 \pm 0.8$ mmol/L, $n_H=0.7$ for HexOH (A3, $n=6$). (B) Summary plots of the logarithm of IC_{50} versus voltage. Solid lines represent the best fits of the function $k(V)=k(0) \times \exp(-zFV/RT)$, where $k(0)$ represents the IC_{50} for 1-alkanols at 0 mV, and z is the fitted value for fractional charges moved during the block. The variables F , R and T have their standard definitions. The fits yield the following model parameters: $k(0)=0.2053$ with $z=-0.4010$ for EtOH; $k(0)=0.0498$ with $z=-0.6217$ for BuOH; and $k(0)=0.0052$ with $z=-0.6999$ for HexOH. (C) Normalized peak current amplitudes are plotted as a function of elapsed time. Currents that were encoded with the mutant I257A and KCNE1 were recorded in the presence of 400 mmol/L EtOH, 200 mmol/L BuOH and 10 mmol/L HexOH, respectively. The membrane potential was depolarized to +60 mV lasting for 3 s. (D) Each average G/G_{max} vs voltage plot with simultaneous fits to the 3-state model for the open channel block (Model II) of I257A with KCNE1 in the presence of various concentrations of EtOH (D1), BuOH (D2) and HexOH (D3). See text for details. The fits correspond to the following parameter values: $K_{OB}=600 \pm 18.5$ mmol/L for EtOH, $K_{OB}=400 \pm 20.1$ mmol/L for BuOH and $K_{OB}=2.9 \pm 3.2$ for HexOH. The error bars indicate the SEM. EtOH, ethanol; BuOH, 1-butanol; HexOH, 1-hexanol.

mmol/L 1-butanol, and 5 mmol/L 1-hexanol, respectively (Figure 2 and 3). Hence, the residue I257 plays a critical role in the inhibition of KCNQ1/KCNE1 channels by 1-alkanols.

The dose-response relationships of I257A also suggest a drastic effect of the residue on KCNQ1 channel sensitivity to 1-alkanols. Figure 5A shows the concentration-dependent effects of all three 1-alkanols on I257A evoked at +20 mV, yielding $IC_{50}=634\pm 0.8$ mmol/L for ethanol ($n=5$), 414 ± 2 mmol/L for 1-butanol ($n=5$) and 7.4 ± 0.8 mmol/L for 1-hexanol ($n=6$), which are much higher than those obtained in the wild-type KCNQ1 channel. As illustrated in Figure 5B, the voltage dependence of IC_{50} was also weaker than that previously described for the wild-type KCNQ1 channels, and the mutation also resulted in the ablation of the closed channel block (Figure 5C). In contrast, we found that an open-channel blocking model (Model II), different from the closed state blocking model (Model I), could adequately fit the responses simultaneously under all circumstances. Taken together, these results suggest that residue I257 plays a key role in the interactions between the 1-alkanols and the closed-state KCNQ1 channel, and the different sensitivities to 1-alkanols in *kqt-3* and KCNQ1 would be due to hydrophobic interactions. In this case, the substitution of I257 by alanine would decrease the hydrophobic forces and thus weaken the inhibitions. In contrast, we found that an open-channel blocking model (Model II), different from the closed state blocking model (Model I), could adequately fit the responses simultaneously under all circumstances (Figure 5D).

Discussion

Alcohol abuse and addiction have been major threats to human health^[37, 38], and drunk driving (ethanol >17 mmol/L as quantified by blood alcohol content) is the largest problem and generates the most social attention.

Alcohol and general anesthetic agents interact with related and relatively specific binding sites in multiple protein targets^[1-3, 7]. Aliphatic alcohols (eg, 1-alkanols) have been used to probe the physicochemical properties of these binding sites^[8]. Findings from these studies are consistent with the presence of physically circumscribed hydrophobic protein cavities that constitute the alcohol and general anesthetic sites.

Amphiphilic binding sites are the foundation of the protein-based theories of alcohol intoxication and general anesthesia that have gained significant recognition in the past. The physiological importance and molecular properties of such active sites have been mainly inferred from the relationship between the narcotic effect and anesthetic solubility, as well as studies with model soluble proteins and theoretical arguments^[24]. Although it is clear that ion channels and other membrane proteins harbor relatively specific and relevant sites for general anesthetic agents, the physicochemical and molecular features of these sites are still not well understood.

In this study, we present the interaction of three members of the homologous series of 1-alkanols with a cloned K⁺ channel KCNQ1; these molecules have been commonly used to study the biological bases of general anesthesia and alcohol action^[8].

In our experiments, the depression of I_{Ks} currents by 1-alkanols revealed that hydrophobic interactions exert a major influence on the interaction between KCNQ1 channels and 1-alkanols. Several studies have suggested that the site of 1-alkanol action was a discrete hydrophobic cleft or pocket, most likely located in the channel polypeptide^[8]. In our case, when ethanol was applied extracellularly, the molecules of ethanol penetrated the cell membrane and blocked the channels through the hydrophobic interaction sites I257 located in the linker of S4-S5.

In addition, the ratio of inhibition in the closed state possessed a larger proportion. The closed-state block demonstrates that the main effect of ethanol block occurs in the first 100 ms, just after the channel is activated, and remains in a stable open state thereafter. In other words, 1-alkanol binding may arise from stabilizing the interface in a configuration that favors the pre-open activated state of the KCNQ1 channel^[39]. This block mechanism was similarly discussed by Christopher J LINGLE, who analyzed the different channel block states of BK channels by several toxins in detail^[32, 33]. Based on the results of the current study, we doubt that there are other amino acids related to the ethanol binding in KCNQ1, as residue I257 was mainly responsible for the closed-state channel block; therefore, some open questions still remain to be answered.

In conclusion, given the unique biophysical properties of KCNQ1, we can relate the inhibition of this channel by 1-alkanols to a possible anesthetic effect. Moreover, the methods described in this study might be used to examine the toxicology of other channels that are candidate targets of ethanol.

Acknowledgements

We are grateful to Dr Bo ZHONG for the critical reading and our colleagues for their comments and discussions. This work was supported by the National Basic Research Program of China (No 2014CB910300), the National Natural Science Foundation of China grants (No 31271209 and 31328007), the Natural Science Foundation of Hubei Province (No 2015CFA095), and Specialized Research Fund for the Doctoral Program of Higher Education of Ministry of Education of China (No 20120142120062); Jing YAO was also supported by university fund (No 2042014KF0230).

Author contribution

Jing YAO and Jiu-ping DING conceived and designed the experiments; Chang XIE, Hao-wen LIU, Na PAN and Jing YAO performed the research, designed the experiments and analyzed the data; Jing YAO, Hao-wen LIU and Jiu-ping DING wrote the paper.

References

- 1 Dopico AM, Anantharam V, Treistman SN. Ethanol increases the activity of Ca²⁺-dependent K⁺ (mslo) channels: functional interaction with cytosolic Ca²⁺. *J Pharmacol Exp Ther* 1998; 284: 258–68.
- 2 Lewohl JM, Wilson WR, Mayfield RD, Brozowski SJ, Morrisett RA, Harris RA. G-protein-coupled inwardly rectifying potassium channels are targets of alcohol action. *Nat Neurosci* 1999; 2: 1084–90.

- 3 Moore MS, Dezaazo J, Luk AY, Tully T, Singh CM, Heberlein U. Ethanol intoxication in *Drosophila*: Genetic and pharmacological evidence for regulation by the cAMP signaling pathway. *Cell* 1998; 93: 997–1007.
- 4 Deitrich RA, Dunwiddie TV, Harris RA, Erwin VG. Mechanism of action of ethanol: initial central nervous system actions. *Pharmacol Rev* 1989; 41: 489–537.
- 5 Homanics GE, Xu Y, Tang P. Integrated approaches to the action of general anesthetics and alcohol. *Physiol Behav* 2002; 77: 495–9.
- 6 Crowder CM. Ethanol targets: a BK channel cocktail in *C elegans*. *Trends Neurosci* 2004; 27: 579–82.
- 7 Covarrubias M, Rubin E. Ethanol selectively blocks a noninactivating K⁺ current expressed in *Xenopus* oocytes. *Proc Natl Acad Sci U S A* 1993; 90: 6957–60.
- 8 Covarrubias M, Vyas TB, Escobar L, Wei A. Alcohols inhibit a cloned potassium channel at a discrete saturable site. Insights into the molecular basis of general anesthesia. *J Biol Chem* 1995; 270: 19408–16.
- 9 Cavaliere S, Gillespie JM, Hodge JJ. KCNQ channels show conserved ethanol block and function in ethanol behaviour. *PLoS One* 2012; 7: e50279.
- 10 Davies AG, Pierce-Shimomura JT, Kim H, VanHoven MK, Thiele TR, Bonci A, et al. A central role of the BK potassium channel in behavioral responses to ethanol in *C elegans*. *Cell* 2003; 115: 655–66.
- 11 Dopico AM, Lemos JR, Treistman SN. Ethanol increases the activity of large conductance, Ca²⁺-activated K⁺ channels in isolated neurohypophysial terminals. *Mol Pharmacol* 1996; 49: 40–8.
- 12 Bukiya AN, Kuntamallappanavar G, Edwards J, Singh AK, Shivakumar B, Dopico AM. An alcohol-sensing site in the calcium- and voltage-gated, large conductance potassium (BK) channel. *Proc Natl Acad Sci U S A* 2014; 111: 9313–8.
- 13 Crowley JJ, Treistman SN, Dopico AM. Cholesterol antagonizes ethanol potentiation of human brain BKCa channels reconstituted into phospholipid bilayers. *Mol Pharmacol* 2003; 64: 365–72.
- 14 Davis SJ, Scott LL, Hu K, Pierce-Shimomura JT. Conserved single residue in the BK potassium channel required for activation by alcohol and intoxication in *C elegans*. *J Neurosci* 2014; 34: 9562–73.
- 15 Dopico AM, Bukiya AN, Martin GE. Ethanol modulation of mammalian BK channels in excitable tissues: molecular targets and their possible contribution to alcohol-induced altered behavior. *Front Physiol* 2014; 5: 466.
- 16 Hu H, Zhou J, Sun Q, Yu XJ, Zhang HL, Ma X, et al. Effects of ethanol on action potential of rat myocardium and human Kv1.5 channel. *Sheng Li Xue Bao* 2011; 63: 219–24.
- 17 Ikeda K, Kobayashi T, Kumanishi T, Yano R, Sora I, Niki H. Molecular mechanisms of analgesia induced by opioids and ethanol: is the GIRK channel one of the keys? *Neurosci Res* 2002; 44: 121–31.
- 18 Hill K G, Alva H, Blednov YA, Cunningham CL. Reduced ethanol-induced conditioned taste aversion and conditioned place preference in GIRK2 null mutant mice. *Psychopharmacology (Berl)* 2003; 169: 108–14.
- 19 Federici M, Nistico R, Giustizieri M, Bernardi G, Mercuri NB. Ethanol enhances GABA_B-mediated inhibitory postsynaptic transmission on rat midbrain dopaminergic neurons by facilitating GIRK currents. *Eur J Neurosci* 2009; 29: 1369–77.
- 20 Michaeli A, Yaka R. Dopamine inhibits GABA(A) currents in ventral tegmental area dopamine neurons via activation of presynaptic G-protein coupled inwardly-rectifying potassium channels. *Neuroscience* 2010; 165: 1159–69.
- 21 Padgett CL, Lalive AL, Tan KR, Terunuma M, Munoz MB, Pangalos MN, et al. Methamphetamine-evoked depression of GABA(B) receptor signaling in GABA neurons of the VTA. *Neuron* 2012; 73: 978–89.
- 22 Trevisani M, Smart D, Gunthorpe MJ, Tognetto M, Barbieri M, Campi B, et al. Ethanol elicits and potentiates nociceptor responses via the vanilloid receptor-1. *Nat Neurosci* 2002; 5: 546–51.
- 23 Vigna SR, Shahid RA, Liddle RA. Ethanol contributes to neurogenic pancreatitis by activation of TRPV1. *FASEB J* 2014; 28: 891–6.
- 24 Kruse SW, Zhao R, Smith DP, Jones DN. Structure of a specific alcohol-binding site defined by the odorant binding protein LUSH from *Drosophila melanogaster*. *Nat Struct Biol* 2003; 10: 694–700.
- 25 Dopico AM. Ethanol sensitivity of BK(Ca) channels from arterial smooth muscle does not require the presence of the beta 1-subunit. *Am J Physiol Cell Physiol* 2003; 284: C1468–C1480.
- 26 Gardner JD, Mouton AJ. Alcohol effects on cardiac function. *Compr Physiol* 2015; 5: 791–802.
- 27 Kanda VA, Purtell K, Abbott GW. Protein kinase C downregulates I_{Ks} by stimulating KCNQ1-KCNE1 potassium channel endocytosis. *Heart Rhythm* 2011; 8: 1641–7.
- 28 Bhuiyan ZA, Wilde AA. I_{Ks} in heart and hearing, the ear can do with less than the heart. *Circ Cardiovasc Genet* 2013; 6: 141–3.
- 29 Rice KS, Dickson G, Lane M, Crawford J, Chung SK, Rees MI, et al. Elevated serum gastrin levels in Jervell and Lange-Nielsen syndrome: a marker of severe KCNQ1 dysfunction? *Heart Rhythm* 2011; 8: 551–4.
- 30 Liu W, Yang J, Hu D, Kang C, Li C, Zhang S, et al. KCNQ1 and KCNH2 mutations associated with long QT syndrome in a Chinese population. *Hum Mutat* 2002; 20: 475–6.
- 31 Yao J, Chen X, Li H, Zhou Y, Yao L, Wu G, et al. BmP09, a "long chain" scorpion peptide blocker of BK channels. *J Biol Chem* 2005; 280: 14819–28.
- 32 Tang QY, Zeng XH, Lingle CJ. Closed-channel block of BK potassium channels by bbTBA requires partial activation. *J Gen Physiol* 2009; 134: 409–36.
- 33 Tang QY, Zhang Z, Xia XM, Lingle CJ. Block of mouse Slo1 and Slo3 K⁺ channels by CTX, IbTX, TEA, 4-AP and quinidine. *Channels (Austin)* 2010; 4: 22–41.
- 34 Klein G, Gardiwal A, Schaefer A, Panning B, Breitmeier D. Effect of ethanol on cardiac single sodium channel gating. *Forensic Sci Int* 2007; 171: 131–5.
- 35 Akiyama T, Yamazaki T, Kawada T, Shimizu S, Suqimachi M, Shirai M. Role of Ca²⁺-activated K⁺ channels in catecholamine release from *in vivo* rat adrenal medulla. *Neurochem Int* 2010; 56: 263–9.
- 36 Difrancesco D. The role of the funny current in pacemaker activity. *Circ Res* 2010; 106: 434–46.
- 37 Foster S, Gmel G, Estevez N, Bahler C, Mohler-Kuo M. Temporal patterns of alcohol consumption and alcohol-related road accidents in young swiss men: seasonal, weekday and public holiday effects. *Alcohol Alcohol* 2015; 50: 565–72.
- 38 He J, Assanangkornchai S, Cai L, McNeil E. Patterns of alcohol consumption in Yunnan province of China: which measure is optimal? *Alcohol Alcohol* 2015; 50: 579–87.
- 39 Bhattacharji A, Kaplan B, Harris T, Qu X, Germann MW, Covarrubias M. The concerted contribution of the S4-S5 linker and the S6 segment to the modulation of a Kv channel by 1-alkanols. *Mol Pharmacol* 2006; 70: 1542–54.